JCTC Journal of Chemical Theory and Computation

ARTICLE

pubs.acs.org/JCTC

Basis Set Dependence of Vibrational Raman and Raman Optical Activity Intensities

James R. Cheeseman* and Michael J. Frisch

Gaussian Inc., 340 Quinnipiac St., Bldg. 40, Wallingford, Connecticut 06492-4050, United States

ABSTRACT: We present a systematic study of the basis set dependence of the backscattering vibrational Raman intensities and Raman Optical Activity (ROA) intensity differences. The accuracies of computed Raman intensities and ROA intensity differences for a series of commonly used basis sets are reported, relative to large reference basis sets, using the B3LYP density functional. This study attempts to separately quantify the relative accuracies obtained from particular basis set combinations: one for the geometry optimization and force field computation and the other for the computation of Raman and ROA tensors. We demonstrate here that the basis set requirements for the geometry and force fields are not similar to those of the Raman and ROA tensors. The Raman and ROA tensors require basis sets with diffuse functions, while geometry optimizations and force field computations typically do not. Eleven molecules were examined: (S)-methyloxirane, (S)-methylthirane, (R)-epichlorhydrin, (S)-CHFClBr, (1S,5S)-α-pinene, (1S,5S)-β-pinene, (1S,4S)-norborneneone, (M)-σ-[4]-helicene, an enone precursor to a cytotoxic sesquiterpene, the gauche−gauche conformer of the monosaccharide methyl-β-D-glucopyranose, and the dipeptide Ac-(alanine)$_2$-NH$_2$. For the molecules examined here, intensities and intensity differences obtained from Raman and ROA tensors computed using the aug-cc-pVDZ basis set are nearly equivalent to those computed with the larger aug-cc-pVTZ basis set. We find that modifying the aug-cc-pVDZ basis set by removing the set of diffuse d functions on all atoms (while keeping the diffuse s and p sets), denoted as aug(sp)-cc-pVDZ, results in a basis set which is significantly faster without much reduction in the overall accuracy. In addition, the popular rDPS basis set introduced by Zuber and Hug offers a good compromise between accuracy and efficiency. The combination of either the aug(sp)-pVDZ or rDPS basis for the computation of the Raman and ROA tensors with the 6-31G* basis set for the geometry optimization and force field calculation is a reliable and cost-effective method for obtaining Raman intensities and ROA intensity differences.

1. INTRODUCTION

Raman optical activity (ROA), the difference in Raman scattering intensity for left and right circularly polarized light, is a powerful tool for studying chiral molecules and determining the structure of biomolecules in their native environment. The theory and first genuine experimental observations of ROA were reported by Barron and Buckingham,[1,2] in the early 1970s. Recent advances in instrumentation[3] and the development of a commercial ROA instrument (the ChiralRAMAN from Bio-Tools, Inc.) have led to an increase in the number of applications. See the review by Barron and Buckingham[4] for the current status of the field. The calculation of ROA spectra using *ab initio* quantum chemical methods is an important aspect of the technique, as comparison of predicted and experimental spectra can provide detailed structural information as well as absolute configuration assignments. There have been many recent computational applications of ROA for a variety of systems, including amino acids,[5,6] small peptides,[6−11] proteins,[12] transition metal complexes,[13] carbohydrates,[14−16] and helicenes[17,18] as well as many other molecules.[19−23] ROA has been used to study atropisomerism in binapthyl derivatives,[24] and recently, the absolute configuration of junionone, a natural monoterpenoid, was determined using ROA.[25] See ref 26 for a review of recent computational applications.

There are several forms of ROA depending on the choice of polarization modulation, scattering geometry, and laser frequency.[27−32] In the far-from-resonance theory, where the exciting laser radiation is far from the lowest allowed electronic excited state, ROA intensity differences depend on the normal mode derivatives of three polarizability tensors, namely, the electric dipole−electric dipole polarizability, the electric dipole−electric quadrupole polarizability, and the electric dipole−magnetic dipole polarizability. The electric dipole−electric dipole polarizability derivatives are used to form two Raman tensor invariants, and all three polarizability derivatives are used to form the three ROA tensor invariants[31,33] from which the Raman intensities and ROA intensity differences are obtained, respectively.

The recent development of fully analytic derivative methods to compute the various polarizability derivatives[34−37] has further extended the size of systems that can be studied. See ref 33 for a review of theoretical approaches for computing ROA intensities. Fully analytic methods offer two choices:[33] a "one-step" procedure in which the force field and Raman/ROA tensor invariants are computed at the same time using the same level of theory and taking advantage of the 2n+1 rule to do only first order CPKS or a "two-step" procedure in which the force field and Raman/ROA tensor invariants are computed in separate steps and require second order CPKS (n+1 rule), thus allowing for the use of different levels of theory for each step. Both procedures require the solution of 11 frequency-dependent first order CPKS equations (three electric, three magnetic, and five quadrupole fields) as well as three times the number of atoms static first order nuclear coordinate CPKS equations. The "two-step" procedure additionally requires the solution of 30 static mixed second order CPKS equations (six electric−electric, nine electric−magnetic, 15 electric−quadrupole). (We note that in Furche's Lagrangian

Received: July 22, 2011
Published: September 13, 2011

approach for computing Raman intensities,[38] the static second order CPKS equations are referred to as "TDKS gradient equations", but the computations involved are identical.) If the basis set requirements for the force field and Raman/ROA tensor invariants are similar, then the "one-step" procedure is optimal, since the additional solution of 30 static CPKS equations is avoided. We note that it is possible to use different levels of theory for the force field and Raman/ROA tensor invariants in an effective "one-step" procedure where the resulting nuclear coordinate derivatives of the three polarizability tensors are combined with a force field computed at a different level of theory. In this case, however, three times the number of atoms static nuclear coordinate CPKS equations need to be solved for each level of theory. Since the number of nuclear coordinate CPKS equations that need to be solved depends on the number of atoms, this step becomes dominant for large molecules. All previous published computational ROA studies have been carried out using a "one-step" procedure or an "effective one-step" procedure as outlined above. Although not addressed in this work, the "two-step" (n+1 rule) has the additional advantage that it allows for alternative approaches to full force-field determination such as mode-tracking[23,39] and intensity-tracking[40,41] methodologies developed by Reiher and co-workers.

Raman intensities are known to be sensitive to diffuse augmentation of the basis set.[38,42] Zuber and Hug[43] have pointed out the importance of diffuse functions in computing ROA tensor invariants. They proposed a minimal rDPS basis set, which is the 3-21++G basis augmented with a semidiffuse p function with an exponent of 0.2 on hydrogen, which provided ROA intensity differences which were close to those obtained using the aug-cc-pVDZ basis set. Although ROA tensor invariants computed using many basis sets were compared in this study, only one basis set was used for the force field. Another basis set study of ROA intensity differences has previously been presented by Ruud and Reiher.[44] They observed comparably good results for the aug-cc-pVDZ and aug-cc-pVTZ basis sets and concluded that the small rDPS basis set proposed by Zuber and Hug[43] was able to reproduce the ROA intensity differences with sufficient accuracy. With the exception of rDPS, ROA intensity differences were obtained from ROA tensors and force fields which were computed using the same basis set. Neither of these studies examined the dependence of the ROA intensity differences on of the level of theory used to compute the optimized geometry and force field. These previous studies also used a numerical procedure for evaluating the nuclear coordinate derivatives of the three polarizability tensors—and were therefore limited to small molecules due to the very demanding computational requirements.

In addition to the quality of the basis set used to compute the Raman/ROA tensor invariants, Raman intensities and ROA intensity differences are also dependent on the quality of the force field via the transformation to normal coordinates. The goal of this study is to separate and quantify these two effects through a systematic study of basis set dependence of the Raman intensities and ROA intensity differences. We examine the dependence of the Raman intensities and ROA intensity differences on the basis set used to compute the Raman/ROA tensors invariants as well as the basis set used for the geometry optimization and force field determination. We also report the relative accuracies of various basis set combinations and address which combinations provide the best accuracy for the cost. Since the purpose of this study is to examine and quantify the basis set convergence of Raman intensities and ROA intensity differences, one functional (B3LYP) is used throughout. Solvent effects and anharmonic corrections are also ignored.

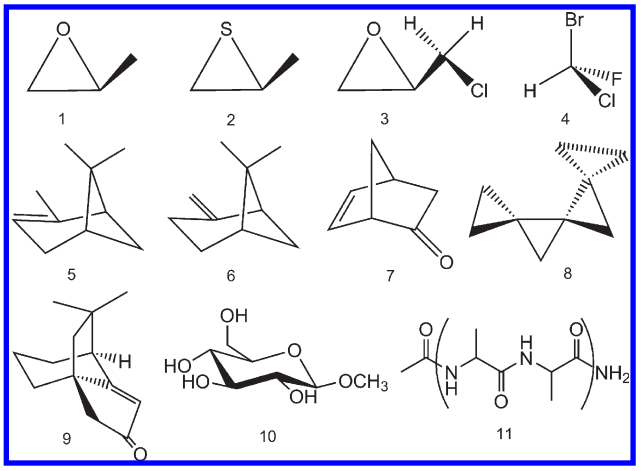

Figure 1. Molecular structures for (S)-methyloxirane (**1**), (S)-methylthirane (**2**), (R)-epichlorhydrin (**3**), (S)-CHFClBr (**4**), (1S,5S)-α-pinene (**5**), (1S,5S)-β-pinene (**6**), (M)-σ-[4]-helicene (**7**), (1S,4S)-norborneneone (**8**), an enone precursor to the cytotoxic sesquiterpene nor-suberosenone (1R,11S)-**9**, methyl-β-D-glucopyranose (**10**), and Ac-(alanine)$_2$-NH$_2$ (**11**).

2. METHODS

The molecules chosen for this study, shown in Figure 1, are (S)-methyloxirane (**1**), (S)-methylthirane (**2**), (R)-epichlorhydrin (lowest energy conformer) (**3**), (S)-CHFClBr (**4**), (1S,5S)-α-pinene (**5**), (1S,5S)-β-pinene (**6**), (M)-σ-[4]-helicene (**7**), (1S,4S)-norborneneone (**8**), an enone precursor to the cytotoxic sesquiterpene nor-suberosenone (1R,11S)-**9**, methyl-β-D-glucopyranose (gauche−gauche conformer) (**10**), and Ac-(alanine)$_2$-NH$_2$ (**11**). Molecules **1**−**3** were chosen because of their small size, thus allowing the use of the large aug-cc-pVQZ basis set as a reference. In addition, they include the second row atoms S and Cl. The ROA spectra has previously been studied, both computationally and experimentally for **1**[44,45] and computationally for **3**.[44,46] Molecule **4** is one of the simplest examples of the (Le Bel and van't Hoff) asymmetric carbon atom. Polavarapu et al.[47] provided the assignment of the absolute configuration on the basis of an *ab initio* ROA spectra calculation. It is included in this study in order to examine the requirement of higher angular momentum diffuse functions. Backscattering ROA measurements[48] and calculated ROA spectra[49] have been previously presented for **5**. For **6**, both forward scattering ROA[50] and backscattering ROA[51] measurements as well as calculated ROA spectra[46] have been presented. Molecule **7** is potentially of interest given the very large value of specific rotation at the sodium D line.[52,53] The ROA spectra of **8** have been measured by Hug et al.,[17] and previous calculations[44,46] have also been presented. Molecule **9**, a chiral enone precursor to the cytotoxic sesquiterpenes nor-suberosenone and nor-suberosanone, was synthesized by Jean-Charles and co-workers[54] and its absolute configuration determined by Stephens and co-workers[55] using VCD. There have been several recent ROA calculations presented for sugars[15,16,56] and carbohydrates.[14] The experimental and calculated Raman and ROA spectra of **10** have been presented previously.[56,57] Given the many recent ROA calculations presented for peptides,[6−12] molecule **11** was chosen as an example peptide model. We note

that eight of the molecules examined here (**1**, **2**, **4**−**9**) are conformationally rigid, and therefore only one conformation is present at room temperature.

The expression for the SCP backscattered Raman intensities ($I^R + I^L$) and ROA intensity differences ($I^R - I^L$) are given by eq 1:

$$I^R + I^L \propto \frac{(\tilde{\nu}_{in} - \tilde{\nu}_i)^4}{1 - \exp[-hc\tilde{\nu}_i/(k_B T)]}[45\alpha_i^2 + 7\beta_i^2]$$

$$I^R - I^L \propto \frac{(\tilde{\nu}_{in} - \tilde{\nu}_i)^4}{1 - \exp[-hc\tilde{\nu}_i/(k_B T)]}[12\beta_{G_i}^2 + 4\beta_{A_i}^2] \quad (1)$$

where

$$\alpha_i^2 = \frac{1}{9}\left(\frac{\partial\alpha_{\alpha\alpha}}{\partial Q_i}\right)_0\left(\frac{\partial\alpha_{\beta\beta}}{\partial Q_i}\right)_0$$

$$\beta_i^2 = \frac{1}{2}\left[3\left(\frac{\partial\alpha_{\alpha\beta}}{\partial Q_i}\right)_0\left(\frac{\partial\alpha_{\alpha\beta}}{\partial Q_i}\right)_0 - \left(\frac{\partial\alpha_{\alpha\alpha}}{\partial Q_i}\right)_0\left(\frac{\partial\alpha_{\beta\beta}}{\partial Q_i}\right)_0\right]$$

$$\beta_{G_i}^2 = \frac{1}{2}\left[3\left(\frac{\partial\alpha_{\alpha\beta}}{\partial Q_i}\right)_0\left(\frac{\partial G'_{\alpha\beta}}{\partial Q_i}\right)_0 - \left(\frac{\partial\alpha_{\alpha\alpha}}{\partial Q_i}\right)_0\left(\frac{\partial G'_{\beta\beta}}{\partial Q_i}\right)_0\right]$$

$$\beta_{A_i}^2 = \frac{\omega}{2}\left[\left(\frac{\partial\alpha_{\alpha\beta}}{\partial Q_p}\right)_0\left(\varepsilon_{\alpha\gamma\delta}\frac{\partial A_{\gamma,\delta\beta}}{\partial Q_p}\right)_0\right] \quad (2)$$

In eqs 1 and 2, α_i^2 and β_i^2 are the Raman invariants, $\beta_{G_i}^2$ and $\beta_{A_i}^2$ are the ROA invariants, and $\tilde{\nu}_{in}$ and $\tilde{\nu}_i$ are the wave numbers of the incident light (532 nm) and of the ith vibrational mode, respectively. Q_i is the normal mode of the ith vibration, and $\alpha_{\alpha\beta}$, $G'_{\alpha\beta}$, and $A_{\alpha\beta\gamma}$ are the frequency dependent electric dipole−electric dipole, electric dipole−magnetic dipole, and electric dipole−electric quadrupole polarizabilities, respectively. Equation 1 includes the ν^4 and Boltzmann factors—which are necessary for comparing calculated spectra to experimental spectra.[22,28,31,44,58,59] Since absolute intensities and intensity differences are not typically measured experimentally, calculated Raman intensities and ROA intensity differences are therefore compared in arbitrary units. We use percent normalized RMS deviations (%NRMS), which is the RMS deviation divided by the range of the reference. For the four smallest molecules (**1**−**4**), the aug-cc-pVQZ basis set was used as a reference for the geometry, force field, Raman, and ROA tensors. For the other molecules (**5**−**11**), the aug-cc-pVTZ basis set was used as a reference for the geometry, force field, and Raman and ROA tensors. We examine the number of wrong signs, within 10% of the range. This provides a more meaningful measure of the quality as only significant wrong signs are seen, thus eliminating small, insignificant values.

3. COMPUTATIONAL DETAILS

All calculations were performed using a development version of Gaussian.[60] The B3LYP functional was used throughout. Frequency dependent ROA and Raman tensors were computed using magnetic field dependent basis functions (GIAOs)[61,62] using either the "one-step" (2n+1) or "two-step" procedure (n+1) algorithm as described by Ruud and Thorvaldsen.[33] The incident light frequency was 532 nm. For the "one-step" procedure, geometry optimization, force field, and Raman and ROA tensors were computed using the same level of theory. For the "two-step" procedure, geometry optimization and the force field computation were carried out in the first step while Raman and ROA tensors were computed in the second step using the geometry and force field obtained from the first step via the checkpoint file. Geometry optimizations used tight convergence criteria where the maximum force was less than 1×10^{-5} au. A pruned (99, 590) grid having 99 radial shells and 590 angular points per shell was used throughout. Raman intensities and ROA intensity differences were computed from the appropriate SCP backscattering combinations of tensor invariants[28,31,33] as in eq 1. Intensities, in arbitrary units, are plotted using a Lorentzian line shape with a half width of 10 cm^{-1}. Percent normalized RMS (%NRMS) is the RMS deviation divided by the range of the reference, multiplied by 100. Modes below 100 cm^{-1} were excluded from the analysis. NWS are the number of wrong signs which have intensity differences ($I^R - I^L$) greater than 10% of the total range of the reference. Tables in the paper include vibrational frequencies in the range 100−1900 cm^{-1}. Differences in the force fields may lead to a different ordering of the vibrational modes, giving rise to apparent differences in the sign of the intensity differences as well as to artificially large %NRMS values. This was particularly the case for the 6-31G* and aug-cc-pVDZ force field basis sets. Care was taken to match corresponding modes, in terms of atomic displacements, in the comparison.

The basis sets used for geometry optimization and force field calculation were aug-cc-pVQZ (molecules **1**−**4** only), aug-cc-pVTZ, cc-pVTZ, 6-31G*, aug-cc-pVDZ, and aug(sp)-cc-pVDZ. The basis sets used to compute Raman/ROA tensors were aug-cc-pVQZ (molecules **1**−**4** only), aug-cc-pVTZ, aug-cc-pVDZ, aug(sp)-cc-pVDZ, rDPS, cc-pVQZ (molecules **1**−**4** only), cc-pVTZ, cc-pVDZ, 6-311++G(2d,2p), 6-311++G**, 6-31G*, TZVP, d-aug-cc-pVTZ, d-aug-cc-pVDZ, and Sadlej and LPol-ds. We use the common convention where the basis set listed before "//" implies the one which was used to compute the Raman and ROA tensors, while the basis set listed after "//" implies the one which was used for the geometry minimization and force field determination. For molecules **1**−**4**, the aug-cc-pVQZ//aug-cc-pVQZ level of theory was used as the reference, and for molecules **5**−**11**, the aug-cc-pVTZ//aug-cc-pVTZ level of theory was used as the reference. For each of the molecules, the numbers of basis functions for many of the basis sets are given in Table 1, along with the number of normal modes considered in the analysis.

The basis set references are as follows. Pople style basis sets: 6-311++G(2d,2p), 6-311++G**, and 6-31G*.[63−70] Dunning's correlation consistent basis sets: cc-pVDZ, cc-pVTZ, and cc-pVQZ.[71] Dunning's singly augmented correlation consistent basis sets: aug-cc-pVDZ, aug-cc-pVTZ, and aug-cc-pVQZ.[72] The d-aug-cc-pVTZ and d-aug-cc-pVDZ[73] are the doubly augmented aug-cc-pVTZ and aug-cc-pVDZ basis sets, respectively. Sadlej basis sets: Sadlej[74,75] and LPol-ds.[76] Ahlrichs' TZVP[77,78] basis set. The rDPS basis set[43] is the 3-21++G basis set augmented with a semidiffuse p function with an exponent of 0.2 on hydrogen. The aug(sp)-cc-pVDZ basis set, introduced here, is obtained from the aug-cc-pVDZ basis set by removing all d type diffuse functions, leaving only s and p type diffuse functions. We note the previous use of pruned augmented basis sets for computing magnetizabilities.[79]

4. RESULTS AND DISCUSSION

4.1. Molecules 1−3. The %NRMS deviations for the frequencies, Raman intensities and ROA intensity differences, and

Table 1. Number of Basis Functions and Normal Modes for Molecules 1−11

molecule	stoichiometry	modes[a]	aug-cc-pVQZ	cc-pVQZ	aug-cc-pVTZ	cc-pVTZ	aug-cc-pVDZ	aug(sp)-cc-pVDZ	rDPS	6-31G*
(**1**) (methyloxirane)	C_3H_6O	18	596	400	322	204	146	126	88	72
(**2**) (methylthirane)	C_3H_6S	18	600	404	326	208	150	121	92	76
(**3**) (epichlorhydrin)	C_3H_5ClO	18	634	429	349	224	164	139	99	89
(**4**) (CHFClBr)	CHFClBr	8	383	267	224	151	118	98	75	81
(**5**) (α-pinene)	$C_{10}H_{16}$	56			828	524	374	324	226	182
(**6**) (β-pinene)	$C_{10}H_{16}$	55[b]			828	524	374	324	226	182
(**7**) (norborneneone)	C_7H_8O	34			552	352	256	216	152	136
(**8**) ((M)-σ-[4]-helicene)	C_8H_{12}	44			690	438	315	270	189	159
(**9**) (enone precursor)	$C_{13}H_{18}O$	71			1058	672	484	414	290	246
(**10**) (β-methyl-glucose)	$C_7H_{14}O_6$	58			920	586	425	360	253	223
(**11**) (Ac-(alanine)$_2$-NH$_2$)	$C_8H_{15}N_3O_3$	59[b]			989	630	457	387	272	240

[a] Number of normal modes between 100 and 1900 cm^{-1}. [b] Number of normal modes between 107 and 1900 cm^{-1}.

the number of wrong signs with respect to those obtained at the aug-cc-pVQZ//aug-cc-pVQZ level of theory for molecules **1**−**3** are given in Table 2, respectively, for various basis set combinations. Deviations of various basis sets used to compute the Raman and ROA tensors using geometries and force fields computed at the aug-cc-pVQZ basis set are presented at the top of the table. The importance of diffuse functions in the basis set used to compute the Raman/ROA tensors is evident. The %NRMS deviation for Raman/ROA tensors computed with the cc-pVQZ basis set is roughly 3−4% for the Raman intensities and 5−7% for the ROA intensity differences, although there are no wrong signs (within 10% of the range of the reference). These results show that even the large quadruple-ζ basis set still benefits from diffuse functions. The %NRMS deviations for the aug-cc-pVTZ basis set are 0.5% or less for both Raman intensities and ROA intensity difference, and there are also no wrong signs. Removing diffuse functions from this triple-ζ basis set (cc-pVTZ) increases the %NRMS deviation to 5−7% for Raman intensities and 10−12% for ROA intensity differences. Also, there is one wrong sign for **1** and **3** and two wrong signs for **2**. This effect is even more dramatic for the double-ζ basis set. The %NRMS deviations for the aug-cc-pVDZ basis set range from less than 1% for Raman intensities and 1−2% for ROA intensity differences. Removing the diffuse functions from this basis set (cc-pVDZ) increases the %NRMS deviation to 7−13% for Raman intensities and to 19−25% for ROA intensity differences and also increases the number of wrong signs. There are two wrong signs for **1**, four wrong signs for **2**, and three wrong signs for **3**. The aug(sp)-cc-pVDZ basis set provides %NRMS deviations for Raman intensities and ROA intensity differences which are close to those obtained using full aug-cc-pVDZ basis set and introduces no wrong signs for these three molecules. The effect of removing the d type diffuse functions increases the Raman intensity %NRMS deviation by roughly 1% while increasing the ROA intensity difference %NRMS by 1−2% . Overall, diffuse d functions have a relatively small influence on the Raman/ROA tensor invariants for molecules **1**−**3** even though **2** contains a sulfur atom and **3** contains a chlorine atom. The small rDPS basis set provides Raman intensity and ROA intensity difference % NRMS deviations which are slightly larger than those of aug(sp)-cc-pVDZ. We note that the rDPS ROA intensity difference % NRMS deviations are slightly less (molecules **1** and **2**) or the same (molecule **3**) as compared to cc-pVQZ. As has previously been shown,[42,43] and is evident from Table 1, 6-31G* is a very poor basis set for computing Raman and ROA tensors. The % NRMS deviations range from 8 to 20% for Raman intensities and 23 to 32% for ROA intensity differences with 2−3 wrong signs introduced.

Although the objective of this study is to examine the basis set convergence of Raman intensities and ROA intensity differences, it is useful to give these %NRMS values some perspective by comparing to the experimental Raman and ROA spectra of **1**. In this case, the experimental Raman and ROA spectra of **1**[80] were scaled, with respect to the spectra obtained at the aug-cc-pVQZ//aug-cc-pVQZ level of theory, by matching the maximum intensity or maximum intensity difference, respectively.[81] The %NRMS deviations, with respect to the experimental spectra, of the Raman intensities and ROA intensity differences obtained at the aug-cc-pVQZ//aug-cc-pVQZ level of theory are roughly 12% and 6%, respectively, and the %NRMS deviation for the frequencies is 2%.

The Raman and ROA spectra for **1** are shown in Figure 2. In this figure, Raman and ROA tensors were computed at each of the aug-cc-pVQZ, aug-cc-pVTZ, aug-cc-pVDZ, aug(sp)-cc-pVDZ, and rDPS basis sets using the aug-cc-pVQZ optimized geometry and force field. The Raman and ROA spectra obtained from the first four basis sets are almost visually indistinguishable. The Raman intensities and ROA intensity differences obtained using the rDPS basis set are overall very similar but show slight intensity increases around 400 cm^{-1} and 950 cm^{-1} in the ROA spectrum.

Raman intensity and ROA intensity difference %NRMS deviations obtained using the reference aug-cc-pVQZ basis set for the Raman and ROA tensors and the aug-cc-pVTZ, cc-pVTZ, 6-31G*, and aug-cc-pVDZ basis sets for the force field are also shown for molecules **1**−**3** in Table 2. Force fields computed at the aug-cc-pVTZ basis provide %NRMS deviations for Raman intensities and ROA intensity differences which differ from aug-cc-pVQZ by 1% or less. Removing the diffuse functions from this triple-ζ basis set (cc-pVTZ) results in %NRMS deviations of Raman intensities and ROA intensity differences which are essentially the same, with the exception of **1** where the ROA % NRMS increases by 2%. Force fields computed using the 6-31G* basis set produce %NRMS deviations of 2−4% for Raman intensities and deviations of 4−6% for ROA intensity differences. There is also one wrong sign introduced for each molecule. Force fields computed using the aug-cc-pVDZ basis set produce % NRMS deviations which are slightly higher than for 6-31G*. There is one wrong sign for **1** and **2**, but no wrong signs for **3**.

Table 2. %RMS Deviations of Frequencies, Raman Intensities, and ROA Intensity Differences of 1−4 for Various Basis Set Combinations[a]

basis set		(1)methyloxirane				(2)methythirane				(3)epichlorhydrin				(4)CHFClBr			
		%NRMS deviation			NWS	%NRMS deviation			NWS	%NRMS deviation			NWS	%NRMS deviation			NWS
force field	Raman/ROA	ν	I^R+I^L	I^R-I^L		ν	I^R+I^L	I^R-I^L		ν	I^R+I^L	I^R-I^L		ν	I^R+I^L	I^R-I^L	
aug-cc-pVQZ:		0.0				0.0				0.0				0.0			
	aug-cc-pVQZ		0.0	0.0	0		0.0	0.0	0		0.0	0.0	0		0.0	0.0	0
	aug-cc-pVTZ		0.2	0.3	0		0.2	0.5	0		0.2	0.4	0		0.6	1.6	0
	aug-cc-pVDZ		0.8	1.2	0		0.8	2.0	0		0.7	1.4	0		2.7	6.3	0
	aug(sp)-cc-pVDZ		1.7	3.5	0		1.6	3.3	0		1.9	3.0	0		13.4	19.4	0
	rDPS		3.2	5.2	0		3.2	4.9	0		4.4	5.5	0		31.7	32.6	1
	cc-pVQZ		2.8	6.0	0		3.2	7.3	0		4.3	5.2	0		8.0	10.6	0
	cc-pVTZ		5.5	11.7	1		4.5	12.2	2		7.2	10.3	1		14.2	17.4	0
	cc-pVDZ		13.1	24.8	2		6.9	20.7	4		11.3	19.0	3		24.7	26.0	0
	6-31G*		19.5	31.9	2		7.6	22.6	2		11.3	25.1	3		18.7	23.0	1
aug-cc-pVTZ:		0.1				0.1				0.2				0.2			
	aug-cc-pVQZ		0.2	1.0	0		1.0	0.6	0		1.2	0.8	0		0.7	0.7	0
	aug-cc-pVTZ		0.3	1.1	0		1.1	0.8	0		1.3	1.0	0		1.0	2.1	0
	aug-cc-pVDZ		0.8	1.6	0		1.3	2.1	0		1.3	1.7	0		3.0	6.9	0
	aug(sp)-cc-pVDZ		1.7	3.8	0		1.3	3.2	0		1.3	3.6	0		13.8	19.9	0
	rDPS		3.2	5.5	0		3.7	4.7	0		5.2	6.1	0		32.3	33.0	2
	6-31G*		19.6	31.3	3		7.6	22.2	2		11.3	25.3	3		19.1	23.1	1
cc-pVTZ:		0.1				0.1				0.1				0.7			
	aug-cc-pVQZ		0.8	3.0	0		0.8	0.8	0		1.3	1.1	0		1.3	1.6	0
	aug-cc-pVTZ		0.8	3.1	0		0.9	1.0	0		1.3	1.3	0		1.6	3.1	0
	aug-cc-pVDZ		0.8	3.5	0		1.1	2.2	0		1.3	1.9	0		3.4	8.0	0
	aug(sp)-cc-pVDZ		1.6	5.2	1		1.4	3.2	0		1.3	3.8	0		14.3	21.7	0
	rDPS		2.9	6.7	1		3.5	4.8	0		5.0	6.2	0		33.0	35.4	2
	cc-pVTZ		5.9	10.9	2		4.2	12.0	3		6.8	10.4	0		14.9	19.3	0
	cc-pVDZ		13.5	23.8	2		6.7	20.3	3		11.2	18.9	1		25.6	28.0	0
	6-311++G(2d,2p)		3.1	8.2	0		1.6	5.7	1		2.8	6.2	0		6.1	12.5	0
	6-311++G**		6.5	17.1	2		2.3	11.4	2		4.9	13.6	2		17.6	23.2	0
	TZVP		9.1	22.3	2		4.4	18.8	4		7.3	16.6	1		28.0	34.7	0
	6-31G*		19.9	30.6	3		7.7	22.0	2		11.2	25.0	3		19.4	24.8	1
6-31G*:		1.2				1.2				1.0				2.2			
	aug-cc-pVQZ		1.9	4.8	1		2.8	5.7	1		3.5	4.1	1		2.0	4.3	0
	aug-cc-pVTZ		1.8	5.0	1		2.9	5.8	1		3.5	4.1	1		2.2	5.8	0
	aug-cc-pVDZ		1.8	5.4	1		3.2	5.9	1		3.2	4.3	1		3.6	10.7	0
	aug(sp)-cc-pVDZ		2.1	7.0	1		3.4	5.4	1		3.2	5.8	1		14.0	24.7	0
	rDPS		3.3	8.8	1		4.9	5.9	1		5.5	8.4	1		32.3	39.5	3
	6-31G*		20.2	34.4	2		8.7	19.0	2		11.6	26.2	3		18.7	28.0	2
aug-cc-pVDZ:		1.2				1.1				1.0				1.3			
	aug-cc-pVQZ		2.8	7.5	1		5.5	6.7	1		3.8	5.9	0		1.1	1.6	0
	aug-cc-pVTZ		2.8	7.5	2		5.7	6.8	1		3.8	6.0	0		1.1	2.2	0
	aug-cc-pVDZ		2.8	7.6	2		6.0	6.9	1		3.9	6.0	0		2.7	5.7	0
	aug(sp)-cc-pVDZ		3.6	9.6	2		5.9	6.5	1		3.0	7.3	1		13.4	17.6	0
aug(sp)-cc-pVDZ:		1.4				1.4				1.2				1.0			
	aug-cc-pVQZ		2.8	6.6	0		6.0	8.0	1		3.8	6.3	1		1.4	1.3	0
	aug-cc-pVDZ		2.7	6.7	0		6.4	8.1	1		4.0	6.6	1		3.3	5.9	0
	aug(sp)-cc-pVDZ		3.4	8.7	0		6.4	8.0	2		3.2	7.9	1		14.3	17.9	0

[a] %NRMS deviations with respect to the aug-cc-pVQZ basis set. NWS is the number of wrong signs within 10% of the range.

Raman and ROA %NRMS deviations obtained using the aug-(sp)-cc-pVDZ for the geometry and force field are similar to those obtained using the aug-cc-pVDZ basis set for **1**, **2**, and **3**. There are also no wrong signs.

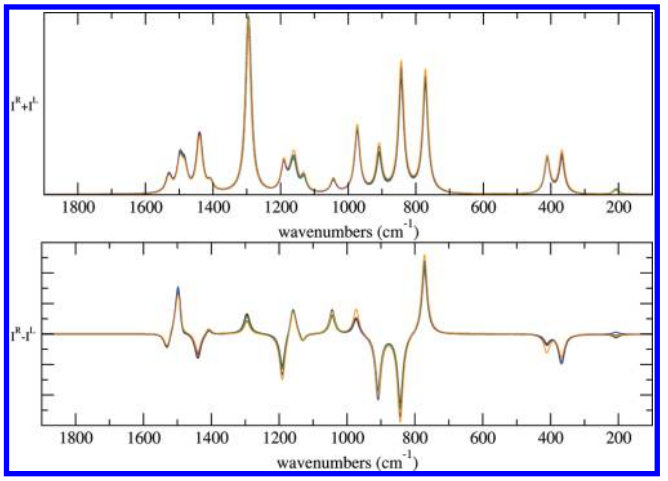

Figure 2. Raman (top) and ROA (bottom) spectra of **1** ((S)-methyloxirane). Geometry and force field computed using aug-cc-pVQZ. ROA tensors computed using aug-cc-pVQZ (black), aug-cc-pVTZ (red), aug-cc-pVDZ (green), aug(sp)-cc-pVDZ (blue), and rDPS (gold).

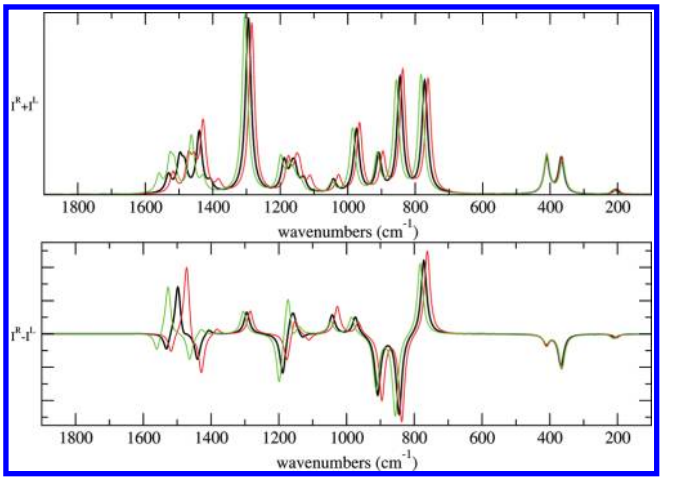

Figure 3. Raman (top) and ROA (bottom) spectra of **1** ((S)-methyloxirane). ROA tensors computed using aug-cc-pVQZ. Geometry and force field computed using cc-pVTZ (black), aug-cc-pVDZ (red), and 6-31G* (green).

The Raman and ROA spectra for **1** for Raman and ROA tensors computed using the aug-cc-pVQZ basis set and geometry and force fields computed using the aug-cc-pVQZ, aug-cc-pVTZ, and cc-pVTZ basis sets are visually indistinguishable and are therefore not shown. The Raman and ROA spectra for **1** for Raman and ROA tensors computed using the aug-cc-pVQZ basis set and geometry and force fields computed using the cc-pVTZ, 6-31G*, and aug-cc-pVDZ basis sets are shown in Figure 3. There are apparent differences. The positions of the frequencies and the relative intensities differ, relative to cc-pVTZ, for 6-31G* and aug-cc-pVDZ starting above 700 cm^{-1}. The 6-31G* basis set provides frequencies which are slightly blue-shifted, relative to cc-pVTZ (and hence aug-cc-pVQZ), while the aug-cc-pVDZ basis set provides frequencies which are slightly red-shifted. Given the similarity of the spectra (**1**) and the small %NRMS deviations between aug-cc-pVTZ and cc-pVTZ (**1**−**3**), diffuse functions appear to have a minimal effect on the geometry and force field for these three molecules.

Also given in Table 2 are the Raman intensity and ROA intensity difference %NRMS deviations for other basis sets used to compute the Raman and ROA tensors using the cc-pVTZ geometry and force field. Note that the Raman and ROA % NRMS deviations are higher for the 6-311++G(2d,2p) basis set, as compared to aug-cc-pVDZ, despite the fact that the former basis set is slightly larger. As pointed out by Wiberg et al.[82] in the context of specific rotations, the Pople style basis sets do not have a diffuse p function on hydrogen, while aug-cc-pVDZ and rDPS do. This appears to be important for Raman and ROA tensors as well. Removing the second set of polarization functions (6-311++G**) causes a dramatic increase in the ROA %NRMS deviation (to 17%, 11%, and 14%, respectively, for molecules **1**−**3**). The extra set of polarization functions appears to partially compensate for the lack of a p type diffuse function on hydrogen. The % NRMS deviations for Raman and ROA tensors obtained using the TZVP basis are also given in Table 2. The TZVP basis set, which lacks diffuse functions, is larger than rDPS and smaller than aug(sp)-cc-pVDZ but gives %NRMS deviations which are only slightly better than those obtained using 6-31G*.

4.2. Molecule 4. The %NRMS deviations for the frequencies, Raman intensities, and ROA intensity differences and number of wrong signs with respect to those obtained at the aug-cc-pVQZ//aug-cc-pVQZ level of theory for molecule **4** are given in Table 2 for various basis set combinations. The importance of diffuse functions in the basis set used to compute the Raman/ROA tensors is even more pronounced than for molecules **1**−**3**. The % NRMS deviation for Raman/ROA tensors computed with the cc-pVQZ basis set is roughly 8% for the Raman intensities and nearly 11% for the ROA intensity differences. These values increase to roughly 25% for the cc-pVDZ basis set. The aug(sp)-cc-pVDZ basis gives a %NRMS deviation for Raman intensities of 13% and ROA intensity differences of nearly 20% compared to 3% and 6%, respectively, for the aug-cc-pVDZ basis set. Clearly diffuse s, p, and d functions are important for **4**. The rDPS basis set, as could be expected, does not perform well for this molecule since there is only one hydrogen and only s and p diffuse functions on F, Cl, and Br. This basis set introduces one wrong sign and gives larger %NRMS deviations than those obtained using the 6-31G* basis set, for both Raman intensities and ROA intensity differences.

Raman intensity and ROA intensity difference %NRMS deviations obtained using the reference aug-cc-pVQZ basis set for the Raman and ROA tensors and the aug-cc-pVTZ, cc-pVTZ, 6-31G*, and aug-cc-pVDZ basis sets for the force field are also shown in Table 2. As was observed for molecules **1**−**3**, the Raman intensities and ROA intensity differences show a relatively small dependence on the presence of diffuse functions in the basis set used to compute the geometry and force field.

4.3. Molecules 5−11. The %NRMS deviations for the frequencies, Raman intensities and ROA intensity differences, and number of wrong signs with respect to those obtained at the aug-cc-pVTZ//aug-cc-pVTZ level of theory are given in Tables 3 and 4 for molecules **5**−**8** and **9**−**11**, respectively, for various basis set combinations. The results for molecules **1**−**4** suggest that this is reasonable given that the Raman and ROA %NRMS deviations obtained from the aug-cc-pVTZ basis set are very similar to those obtained using the much larger quadruple-ζ basis set aug-cc-pVQZ.

Deviations of various basis sets used to compute the Raman and ROA tensors using geometries and force fields computed using the aug-cc-pVTZ basis set are presented at the top of Tables 3 and 4. Again, the importance of diffuse functions for the

Table 3. %RMS Deviations of Frequencies, Raman Intensities, and ROA Intensity Differences of Molecules 5−8 for Various Basis Set Combinations[a]

		(5)α-pinene				(6)β-pinene				(7)norborneneone				(8)(M)-σ-[4]-helicene			
basis set		%NRMS deviation			NWS	%NRMS deviation			NWS	%NRMS deviation			NWS	%NRMS deviation			NWS
force field	Raman/ROA	ν	I^R+I^L	I^R-I^L		ν	I^R+I^L	I^R-I^L		ν	I^R+I^L	I^R-I^L		ν	I^R+I^L	I^R-I^L	
aug-cc-pVTZ:		0.0				0.0				0.0				0.0			
	aug-cc-pVTZ		0.0	0.0	0		0.0	0.0	0		0.0	0.0	0		0.0	0.0	0
	aug-cc-pVDZ		0.3	0.5	0		0.2	0.5	0		0.4	0.4	0		0.2	0.4	0
	aug(sp)-cc-pVDZ		0.5	1.0	0		0.4	0.8	0		1.8	1.3	0		0.4	1.0	0
	rDPS		1.1	1.8	0		1.9	1.6	0		3.6	2.3	0		1.2	2.7	1
cc-pVTZ:		0.1				0.1				0.1				0.1			
	aug-cc-pVTZ		0.1	0.5	0		0.3	0.6	0		0.6	0.4	0		0.2	0.3	0
	aug-cc-pVDZ		0.3	0.7	0		0.3	0.7	0		0.8	0.7	0		0.2	0.5	0
	aug(sp)-cc-pVDZ		0.5	1.1	0		0.6	1.0	0		1.9	1.4	0		0.4	1.1	0
	rDPS		1.1	1.9	0		1.9	1.8	0		3.7	2.4	0		1.2	2.7	0
	cc-pVTZ		3.2	6.5	0		5.6	7.8	1		7.8	4.9	0		3.6	7.2	1
	cc-pVDZ		6.7	15.0	3		8.5	15.4	3		11.8	9.5	1		6.6	15.4	1
	6-311++G(2d,2p)		0.6	1.9	0		0.6	1.7	0		1.2	1.0	0		0.4	1.3	0
	6-311++G**		1.7	4.9	0		1.1	4.6	0		2.8	2.3	0		1.1	2.9	0
	TZVP		3.4	9.1	1		4.5	9.7	2		6.6	5.4	0		3.4	6.3	1
	6-31G*		10.3	22.3	10		10.1	20.4	6		13.6	12.1	1		8.3	21.5	1
6-31G*:		1.0				1.0				0.8				0.9			
	aug-cc-pVTZ		1.1	4.4	1		1.8	4.9	2		3.1	1.6	0		1.7	2.3	0
	aug-cc-pVDZ		1.1	4.3	1		1.8	4.8	2		3.2	1.8	0		1.8	2.3	0
	aug(sp)-cc-pVDZ		1.0	4.9	1		2.0	5.0	2		3.9	2.6	0		1.8	2.6	0
	rDPS		1.4	5.0	1		2.9	5.1	2		5.1	3.1	0		2.4	3.6	0
	6-31G*		10.2	28.7	9		10.3	20.1	7		14.1	12.9	1		9.0	22.1	4
aug-cc-pVDZ:		0.6				0.6				0.6				0.7			
	aug-cc-pVTZ		4.9	10.3	2		2.3	4.4	1		5.7	3.1	0		1.6	3.4	1
	aug-cc-pVDZ		4.9	10.2	2		2.2	4.3	1		5.7	3.3	0		1.7	3.5	1
	aug(sp)-cc-pVDZ		4.8	10.5	2		2.3	4.4	1		6.0	3.6	0		1.6	3.7	1
aug(sp)-cc-pVDZ:		0.9				0.9				0.7				1.3			
	aug-cc-pVDZ		3.3	8.8	3		2.5	4.6	3		3.1	3.4	0		2.6	3.6	0
	aug(sp)-cc-pVDZ		3.2	8.8	2		2.4	4.9	3		3.8	4.0	0		2.2	3.7	0

[a] %NRMS deviations with respect to the aug-cc-pVTZ basis set. NWS is the number of wrong signs within 10% of the range.

Raman/ROA tensors is evident. The %NRMS deviations for Raman intensities and ROA intensity differences for molecules **5**−**11** show trends similar to those for **1**−**4**. Raman and ROA tensors computed using the aug-cc-pVDZ basis set provide % NRMS deviations for both Raman intensities and ROA intensity differences that differ from those obtained using the aug-cc-pVTZ basis set by less than 1%. There are also no wrong signs. The aug(sp)-cc-pVDZ basis set provides %NRMS deviations for Raman intensities and ROA intensity differences which are close to those obtained using full aug-cc-pVDZ basis set and introduces no wrong signs for these seven molecules. The effect of removing the d type diffuse functions increases both the Raman intensity and ROA intensity difference %NRMS deviations by less than 2%. With the exception of **10**, the small rDPS basis set provides Raman intensity and ROA intensity difference %NRMS deviations which are a few percent larger than those of aug(sp)-cc-pVDZ.

The Raman and ROA spectra for **5** are shown in Figure 4, and the ROA spectra of **9** are shown at the top of Figure 6. In these figures, the Raman and ROA tensors were computed at each of the aug-cc-pVTZ, aug-cc-pVDZ, aug(sp)-cc-pVDZ, and rDPS basis sets using the aug-cc-pVTZ optimized geometry and force field. The Raman and ROA spectra obtained from the these basis sets are almost visually indistinguishable.

Raman intensity and ROA intensity difference %NRMS deviations obtained using the reference aug-cc-pVTZ basis set for the Raman and ROA tensors and each of the cc-pVTZ, 6-31G*, and aug-cc-pVDZ basis sets for the force field are also given in Tables 3 and 4 for molecules **5**−**8** and **9**−**11**, respectively. For molecules **5**−**9**, force fields computed using the cc-pVTZ basis set provide %NRMS deviations for Raman intensities and ROA intensity differences which differ from aug-cc-pVTZ by 1% or less. These values are higher for molecules **10** and **11**. For molecules **5**−**9**, force fields computed using the 6-31G* basis set produce %NRMS deviations of 1−3% for Raman intensities and deviations of 2−5% for ROA intensity differences. Again, these values are higher for molecules **10** and **11**, where the Raman intensity %NRMS deviations are 8% and 7%, respectively, and the ROA intensity difference %NRMS deviations are 11% and 7%, respectively. With the exception of molecules **10** and **11**, force fields computed using either the aug-cc-pVDZ or aug(sp)-cc-pVDZ basis

Table 4. %RMS Deviations of Frequencies, Raman Intensities, and ROA Intensity Differences of Molecules 9−11 for Various Basis Set Combinations[a]

basis set		(9)enone				(10)methyl-β-D-glucose (gg)				(11)Ac-(alanine)$_2$-NH$_2$			
		%NRMS deviation			NWS	%NRMS deviation			NWS	%NRMS deviation			NWS
force field	Raman/ROA	ν	I^R+I^L	I^R-I^L		ν	I^R+I^L	I^R-I^L		ν	I^R+I^L	I^R-I^L	
aug-cc-pVTZ:		0.0				0.0				0.0			
	aug-cc-pVTZ		0.0	0.0	0		0.0	0.0	0		0.0	0.0	0
	aug-cc-pVDZ		0.1	0.5	0		0.3	0.7	0		0.6	0.5	0
	aug(sp)-cc-pVDZ		0.1	1.2	0		1.6	2.5	0		1.9	1.4	0
	rDPS		1.0	2.4	0		6.0	8.6	1		3.7	4.4	0
cc-pVTZ:		0.1				0.2				0.2			
	aug-cc-pVTZ		0.6	0.5	0		1.5	2.9	0		2.9	3.6	0
	aug-cc-pVDZ		0.6	0.7	0		1.6	2.9	0		3.1	3.7	0
	aug(sp)-cc-pVDZ		0.6	1.1	0		2.5	3.4	0		3.5	4.6	0
	rDPS		1.4	2.3	0		6.3	8.5	2		4.8	7.3	0
	cc-pVTZ		2.7	5.4	0		6.9	11.6	4		8.4	7.4	0
	cc-pVDZ		4.1	15.0	4		12.9	19.3	10		14.5	13.8	4
	6-311++G(2d,2p)		0.7	1.2	0		2.5	4.4	0		3.4	4.1	0
	6-311++G**		0.6	3.6	0		3.8	6.9	0		4.5	5.9	0
	TZVP		2.0	7.1	0		7.6	14.1	4		8.8	8.4	1
	6-31G*		4.2	24.3	8		15.9	25.0	10		19.0	17.3	6
6-31G*:		0.9				1.3				1.1			
	aug-cc-pVTZ		1.4	3.4	1		7.8	10.9	1		6.8	7.1	1
	aug-cc-pVDZ		1.4	3.4	1		8.2	11.0	1		7.0	7.1	1
	aug(sp)-cc-pVDZ		1.4	3.4	1		8.3	12.6	1		7.4	8.1	2
	rDPS		1.8	3.9	1		10.4	19.1	3		8.2	10.5	2
	6-31G*		4.3	25.2	7		17.6	37.1	9		19.2	18.7	8
aug-cc-pVDZ:		0.5				1.5				0.7			
	aug-cc-pVTZ		1.4	6.6	4		3.2	3.3	0		6.5	4.5	1
	aug-cc-pVDZ		1.4	6.6	4		3.2	3.5	0		6.6	4.6	1
	aug(sp)-cc-pVDZ		1.4	7.0	4		3.6	4.7	0		7.0	4.9	1
aug(sp)-cc-pVDZ:		0.8				0.8				0.9			
	aug-cc-pVDZ		1.7	7.4	1		3.3	3.7	0		6.0	4.6	0
	aug(sp)-cc-pVDZ		1.7	7.8	2		3.7	4.8	0		6.4	5.0	1

[a] %NRMS deviations with respect to the aug-cc-pVTZ basis set. NWS is the number of wrong signs within 10% of the range.

sets produce %NRMS deviations which are the same or higher than those for 6-31G*. These results indicate that molecules **10** and **11** are more sensitive to the presence of diffuse functions in the basis set used to compute the force field.

The dependence of the Raman (for molecule **5**) and ROA (for molecules **5** and **9**) spectra on the basis set used for the geometry and force field are shown in Figure 5 and at the bottom of Figure 6, respectively. As can be observed in these figures, the Raman and ROA spectra computed using the aug-cc-pVTZ and cc-pVTZ basis sets are visually indistinguishable. The positions of the frequencies and the relative intensities differ, relative to aug-cc-pVTZ (or cc-pVTZ), for 6-31G* and aug-cc-pVDZ starting above 700 cm^{-1}. The 6-31G* basis set provides frequencies which are slightly blue-shifted, while the aug-cc-pVDZ basis set provides frequencies which are slightly red-shifted.

Also given in Tables 3 (molecules **5**−**8**) and 4 (molecules **9**−**11**) are the Raman intensity and ROA intensity difference %NRMS deviations for other basis sets used to compute the Raman and ROA tensors using the cc-pVTZ geometry and force field. The same trends can be observed as for molecules **1**−**3**.

The Sadlej basis set[74,75] has been shown to yield Raman intensities[42] and ROA intensity differences[43,44] of a quality close to aug-cc-pVTZ. Raman intensity and ROA intensity difference %NRMS deviations for the Sadlej basis set were found to be equivalent (within 1%) to the aug-cc-pVTZ deviations and are therefore not shown. The large LPol-ds basis set of Sadlej[76] has been shown to correctly predict the sign and magnitude of the optical rotation for **6** (β-pinene) at long wavelengths and to significantly improve the short wavelength prediction, as compared to aug-cc-pVDZ and aug-cc-pVTZ. However, Raman and ROA %NRMS deviations computed using the LPol-ds basis set were found to be essentially equivalent to those obtained using the aug-cc-pVTZ basis set and are likewise not shown. Raman intensity and ROA intensity difference %NRMS deviations obtained using the (doubly augmented) d-aug-cc-pVTZ basis set were found to be the same as those obtained with the aug-cc-pVTZ basis set. The (doubly augmented) d-aug-cc-pVDZ basis set gave Raman intensity and ROA intensity difference %NRMS deviations which were either slightly closer to those obtained with aug-cc-pVTZ or the same as aug-cc-pVDZ.

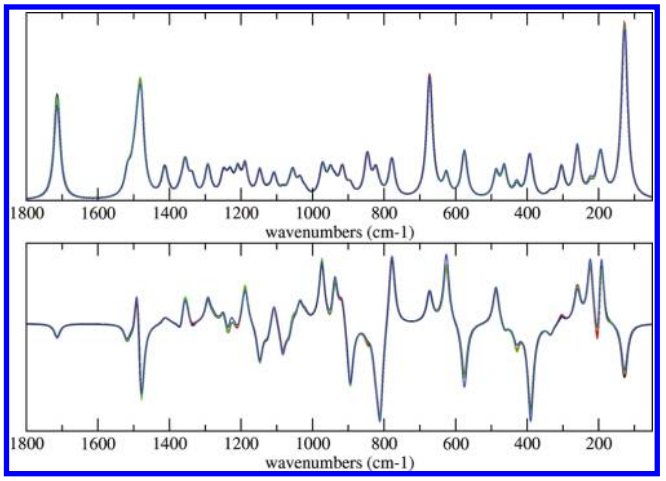

Figure 4. Raman (top) and ROA (bottom) spectra of **5** ((1S,5S)-α-pinene). Geometry and force field computed using aug-cc-pVTZ. ROA tensors computed using aug-cc-pVTZ (black), aug-cc-pVDZ (red), aug(sp)-cc-pVDZ (green), and rDPS (blue).

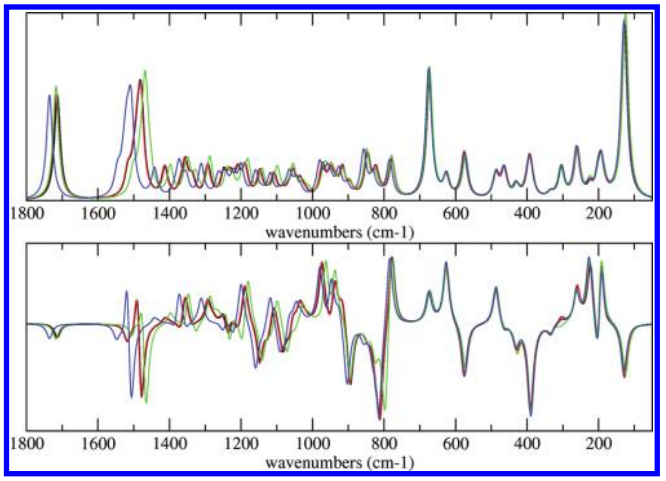

Figure 5. Raman (top) and ROA (bottom) spectra of **5** ((1S,5S)-α-pinene). ROA tensors computed using aug-cc-pVTZ. Geometry and force field computed using aug-cc-pVTZ (black), cc-pVTZ (red), aug-cc-pVDZ (green), and 6-31G* (blue).

4.4. Timing Differences between the "One-Step" and "Two-Step" Procedures. Relative timings for the various basis combinations are given in Table 5 for molecule **9**, the largest molecule examined here. Timings in this table assume 100 CPU units for the aug-cc-pVTZ//aug-cc-pVTZ level of theory. Data are given with and without accounting for the geometry optimization time, which assumes nine steps. Compared to the aug-cc-pVTZ//aug-cc-pVTZ level of theory, the aug-cc-pVDZ//cc-pVTZ combination reduces the amount of CPU time by more than a factor of 10. The aug-cc-pVDZ//6-31G* combination reduces time by roughly factor of 20, while the aug(sp)-cc-pVDZ//6-31G* combination reduces the time by more than a factor of 30. When the geometry optimization step is included, the aug(sp)-cc-pVDZ//6-31G* combination reduces the CPU time by a factor of 40, relative to aug-cc-pVTZ//aug-cc-pVTZ. The aug(sp)-cc-pVDZ basis set provides nearly a factor of 2 reduction in cost over the aug-cc-pVDZ basis set for computing just the Raman/ROA tensors via the "two-step" procedure. The time to compute both Raman intensities and ROA intensity differences using the aug-cc-pVDZ//6-31G* combination is essentially the same as the aug-cc-pVDZ//aug-cc-pVDZ combination (obtained via the "one-step" procedure), not including the geometry optimization step. However, when the geometry optimization step is included, the aug-cc-pVDZ//6-31G* combination shows a slight advantage. This is also the case with aug(sp)-cc-pVDZ//6-31G* and aug(sp)-cc-pVDZ//aug(sp)-cc-pVDZ. This difference will increase with the size of the molecule, and also if more geometry

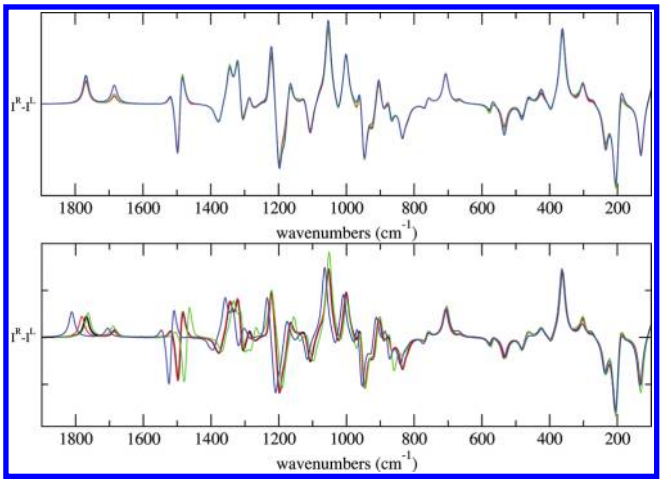

Figure 6. ROA spectra of **9**. Top: Geometry and force field computed using aug-cc-pVTZ. ROA tensors computed using aug-cc-pVTZ (black), aug-cc-pVDZ (red), aug(sp)-cc-pVDZ (green), and rDPS (blue). Bottom: ROA tensors computed using aug-cc-pVTZ. Geometry and force field computed using aug-cc-pVTZ (black), cc-pVTZ (red), aug-cc-pVDZ (green), and 6-31G* (blue).

Table 5. Relative Timings for Various Basis Set Combinations for Molecule 9[a]

basis set			
force field	Raman/ROA	time	time (including geom. opt)[b]
aug-cc-pVTZ:			
	aug-cc-pVTZ[c]	100.0	100.0
cc-pVTZ:			
	aug-cc-pVDZ	9.5	9.8
	aug(sp)-cc-pVDZ	7.1	7.7
	rDPS	5.3	6.3
6-31G*:			
	aug-cc-pVDZ	5.4	4.6
	aug(sp)-cc-pVDZ	3.0	2.5
	rDPS	1.2	1.1
aug-cc-pVDZ:			
	aug-cc-pVDZ[c]	5.5	5.8
	aug-cc-pVDZ	7.8	7.7
aug(sp)-cc-pVDZ:			
	aug(sp)-cc-pVDZ[c]	3.1	3.3
	aug(sp)-cc-pVDZ	4.2	4.2

[a] Time to compute just the Raman/ROA tensors using the "two-step" procedure: aug-cc-pVDZ = 5.1; aug(sp)-cc-pVDZ = 2.7; rDPS = 0.9. [b] Assuming nine optimization steps. [c] Computed using the "one-step" procedure.

Table 6. %NRMS Deviations of ROA Intensity Differences with and without the Electric-Dipole−Electric-Quadrupole Contribution[a]

	ref	aug(sp)-cc-pVDZ//6-31G*			
	$I^R - I^L$	$I^R - I^L$	NWS	$I^R - I^L$	NWS
molecule	(without EQ)	(including EQ)		(without EQ)	
(**1**) (methyloxirane)	3.1	7.0	1	5.9	1
(**2**) (methylthirane)	2.1	8.1	1	7.2	1
(**3**) (epichlorhydrin)	2.7	5.9	1	4.8	1
(**4**) (CHFClBr)	2.0	24.8	0	25.8	1
(**5**) (α-pinene)	2.9	4.9	1	4.4	1
(**6**) (β-pinene)	3.2	5.0	2	5.5	2
(**7**) (norborneneone)	1.7	2.6	0	2.0	0
(**8**) ((M)-σ-[4]-helicene)	3.2	2.6	0	4.2	0
(**9**) (enone precursor)	3.7	3.4	1	5.1	0
(**10**) (β-methyl-glucose)	3.8	13.5	3	12.0	3
(**11**) (Ac-(alanine)$_2$-NH$_2$)	3.0	8.1	2	7.9	2

[a] aug-cc-pVQZ//aug-cc-pVQZ for molecules **1**−**4**. aug-cc-pVTZ//aug-cc-pVTZ for molecules **5**−**11**.

optimization steps are required (i.e., floppy molecules). The aug(sp)-cc-pVDZ//6-31G* combination provides roughly a factor of 2 reduction in cost over the aug-cc-pVDZ//6-31G* combination, including the geometry optimization step. The rDPS/6-31G* combination provides roughly a factor of 4 reduction over aug-cc-pVDZ//6-31G*, including the geometry optimization steps. The aug(sp)-cc-pVDZ//6-31G* and rDPS//6-31G* combinations would become even more advantageous for larger molecules.

4.5. Electric-Dipole−Electric-Quadrupole Contribution. Luber et al.[46] examined the importance of the electric-dipole−electric-quadrupole contribution to ROA intensity differences ($\beta_{A_i}{}^2$ in eqs 1 and 2). With the exception of some C−H stretching vibrations, they found the electric-dipole−electric-quadrupole contribution to the SCP backscattering ROA intensity differences to be small. They found that neglecting the electric-dipole−electric-quadrupole tensor resulted in an overall small change to the spectra below 2000 cm^{-1}. (Molecules **1** (methyloxirane), **3** (epichlorhydrin), **6** (β-pinene), and **8** ((M)-σ-[4]-helicene) were included in their study.) Neglecting the electric-dipole−electric-quadrupole contribution reduces the number of CPKS equations from 41 to 21 for the "two-step" procedure (and from 11 to 6 for the "one-step" procedure). Although the number of CPKS equations is reduced by nearly a factor of 2, this results in only a modest speedup (roughly 1.4 for molecule **9**) in computing the Raman and ROA tensors using the "two-step" procedure.

The effect of neglecting the electric-dipole−electric-quadrupole contribution on the ROA intensity difference %NRMS deviations is shown in Table 6. For molecules **1**−**4**, excluding the electric-dipole−electric-quadrupole contribution gives a %NRMS deviation for the ROA intensity differences of 2−3%, with respect to aug-cc-pVQZ//aug-cc-pVQZ level of theory. For molecules **5**−**11**, the %NRMS deviation is 2−4% with respect to aug-cc-pVTZ//aug-cc-pVTZ. Interestingly, the %NRMS deviation obtained from excluding the electric-quadrupole contribution becomes slightly less than the %NRMS, which includes this contribution at the aug(sp)-cc-pVDZ//6-31G* level of theory for molecules **1**−**3**, **5**, **8**, **10**, and **11**. For molecules **6**, **7**, and **9**, the %NRMS deviation obtained from excluding the electric-quadrupole contribution is just slightly larger. Although not shown, this same trend is observed at the rDPS//6-31G* level of theory. On the basis of these limited results (and those of ref 46), neglecting the electric-dipole−electric-quadrupole tensor contribution appears to be a reasonable approximation for computing SCP backscattering ROA spectra, especially when applied to large molecules where the aug(sp)-cc-pVDZ//6-31G* or rDPS//6-31G* level of theory is practical. It remains to be seen if this is, in fact, general.

5. CONCLUSIONS

In this study, we have conducted a systematic investigation of the basis set dependence of the backscattering vibrational Raman intensities and Raman Optical Activity (ROA) intensity differences. We have separately quantified the basis set dependence of the Raman/ROA tensor invariants and the force field on the resulting Raman intensities and ROA intensity differences. We observe that the basis set requirements for Raman/ROA tensor invariants and the force field are not similar. Raman/ROA tensor invariants require basis sets with diffuse functions while geometry optimizations and force field calculations typically do not. Given these observations, we conclude that the "two-step" procedure (n+1 rule) is more efficient than the "one-step" procedure (2n+1 rule) for computing accurate Raman intensities and ROA intensity differences, especially for large molecules.

Raman/ROA tensor invariants computed using the aug-cc-pVTZ basis set provide Raman intensities and ROA intensity differences which are essentially equivalent to those obtained using the much larger aug-cc-pVQZ basis set (for molecules **1**−**4**). More importantly, Raman intensities and ROA intensity differences obtained using the aug-cc-pVDZ basis set for the Raman/ROA tensor invariants are of nearly the same quality as those obtained using the aug-cc-pVTZ basis set. We find that modifying the aug-cc-pVDZ basis set by removing the set of diffuse d functions (while keeping the diffuse s and p sets) results in a basis set, denoted as aug(sp)-cc-pVDZ, which is significantly faster without much loss in the overall accuracy. In addition, we find that the popular rDPS basis set introduced by Zuber and Hug[43] offers a good compromise between accuracy and cost.

Geometries and force fields computed using the cc-pVTZ basis set provide Raman intensities and ROA intensity differences which are essentially equivalent to those obtained using the aug-cc-pVTZ basis, which are in turn are nearly equivalent to those obtained using the aug-cc-pVQZ basis set (for molecules **1**−**4**). At least for the types of molecules examined here, geometries and force fields computed at the aug-cc-pVTZ basis set offer no additional advantage over cc-pVTZ. Geometries and force fields computed using the 6-31G* basis set provide Raman intensities and ROA intensity differences which are less accurate, but still acceptable. With the exception of **10** and **11**, the 6-31G* basis set (for the force field determination) provides Raman intensities and ROA intensity differences which are the same or better than those of aug-cc-pVDZ. The aug(sp)-cc-pVDZ basis set is slightly less accurate but still provides reasonable results. The 6-31G* basis set offers a significant computational advantage for geometry optimizations and force field calculations, especially for large molecules, where the geometry optimization step can require a significant amount of computational time (on the same order as computing the force field), especially if the molecule has multiple low energy conformations which need to be explored.

If one assumes nine optimization steps, geometry optimization takes roughly one-half of the time required to compute the frequencies for molecule **9**.

For small molecules, we recommend the aug-cc-pVDZ basis for computing the Raman/ROA tensor invariants combined with geometry optimizations and force fields computed using the cc-pVTZ basis set (aug-cc-pVDZ//cc-pVTZ level of theory), for intermediate size molecules, aug(sp)-cc-pVDZ//cc-pVTZ or rDPS//6-31G*, and for large molecules, either the aug(sp)-cc-pVDZ//6-31G* or rDPS//6-31G* levels of theory. If the "one-step" procedure is the only option, then the aug-cc-pVDZ//aug-cc-pVDZ or aug(sp)-cc-pVDZ//aug(sp)-cc-pVDZ levels of theory offer the only reasonable choice. Raman/ROA tensor invariants computed using either the aug(sp)-cc-pVDZ or smaller rDPS basis sets, in combination with the geometry optimizations and force fields computed using the 6-31G* basis set, are a reasonable choice in terms of accuracy versus cost and should be applicable to the study of molecules such as peptides, proteins, carbohydrates, and natural products.

AUTHOR INFORMATION

Corresponding Author

*E-mail: cheese@gaussian.com.

ACKNOWLEDGMENT

The authors would like to thank Professor Larry Nafie (Syracuse University and Biotools) and Dr. Hank Lee (Biotools) for kindly providing the experimental Raman and ROA spectra of **1**.

REFERENCES

(1) Barron, L. D.; Buckingham, A. D. *Mol. Phys.* **1971**, *20*, 1111.
(2) Barron, L.; Bogaard, M. P.; Buckingham, A. D. *J. Am. Chem. Soc.* **1973**, *95*, 603.
(3) Hug, W.; Hangartner, G. A. *J. Raman Spectrosc.* **1999**, *30*, 841–852.
(4) Barron, L.; Buckingham, A. D. *Chem. Phys. Lett.* **2010**, *492*, 199–213.
(5) Pecul, M. *Chem. Phys. Lett.* **2006**, *427*, 166–176.
(6) Jalkanen, K. J.; Degtyarenko, I. M.; Neiminen, R. M.; Cao, X.; Nafie, L. A.; Zhu, F.; Barron, L. *Theor. Chem. Acc.* **2008**, *119*, 191–210.
(7) Herrmann, C.; Ruud, K.; Reiher, M. *ChemPhysChem* **2006**, *7*, 2189–2196.
(8) Jacob, C. R.; Luber, S.; Reiher, M. *J. Phys. Chem. B* **2009**, *113*, 6558–6573.
(9) Jacob, C. R.; Luber, S.; Reiher, M. *Chem.—Eur. J.* **2009**, *15*, 13491–13508.
(10) Mukhopadhyay, P.; Zuber, G.; Beratan, D. N. *Biophys. J.* **2008**, *95*, 5574–5586.
(11) Kapitán, J.; Fujiang, Z.; Hecht, L.; Gardiner, J.; Seebach, D.; Barron, L. *Angew. Chem., Int. Ed.* **2008**, 47.
(12) Luber, S.; Reiher, M. *J. Phys. Chem. B* **2010**, *114*, 1057–1063.
(13) Luber, S.; Reiher, M. *Chem. Phys.* **2008**, *346*, 212–223.
(14) Macleod, N. A.; Johannessen, C.; Hecht, L.; Barron, L.; Simons, J. P. *Int. J. Mass Spectrom.* **2006**, *253*, 193–200.
(15) Luber, S.; Reiher, M. *J. Phys. Chem. A* **2009**, *113*, 8268–8277.
(16) Kaminský, J.; Kapitán, J.; Baumruk, V.; Bednárová, L.; Bouř, P. *J. Phys. Chem. A.* **2009**, 3594–3601.
(17) Hug, W.; Zuber, G.; de Meijere, A.; Khlebnikov, A. F.; Hansen, H.-J. *Helv. Chim. Acta* **2001**, *84*, 1–21.
(18) Liégeois, V.; Champagne, B. *J. Comput. Chem.* **2008**, *30*, 1261–1278.
(19) Kapitán, J.; Johannessen, C.; Bouř, P.; Hecht, L.; Barron, L. *Chirality* **2009**, *21*, E4–E12.
(20) Fedorovsky, M.; Gerlach, H.; Hug, W. *Helv. Chim. Acta* **2009**, *92*, 1451–1465.
(21) Liégeois, V.; Quinet, O.; Champagne, B.; Haesler, J.; Zuber, G.; Hug, W. *Vib. Spectrosc.* **2006**, *42*, 309–316.
(22) Hug, W.; Haesler, J. *Int. J. Quantum Chem.* **2005**, *104*, 695–715.
(23) Herrmann, C.; Neugebauer, J.; Reiher, M. *New J. Chem.* **2007**, *31*, 818–831.
(24) Liégeois, V. *ChemPhysChem* **2009**, *10*, 2017–2025.
(25) Lovchik, M. A.; Frater, G.; Goeke, A.; Hug, W. *Chem. Biodivers.* **2008**, *5*, 126–139.
(26) Pecul, M. *Chirality* **2009**, *21*, E98–E104.
(27) Hecht, L.; Nafie, L. A. *Mol. Phys.* **1991**, *72*, 441–469.
(28) Nafie, L. A.; Che, D. In *Modern Nonlinear Optics, Part 3*; Evans, M., Kielich, S., Eds.; Wiley: New York, 1994; Advances in Chemical Physics Vol. 85, pp 105−149.
(29) Nafie, L. A. *Annu. Rev. Phys. Chem.*; Annual Reviews, Inc.: Palo Alto, CA, 1997; Vol. 48, pp 357−386.
(30) Nafie, L. A. In *Encyclopedia of Spectroscopy and Spectrometry*; Tranter, G., Holmes, J., Lindon, J., Eds.; Academic Press: London, 2000; pp 1976−1985.
(31) Barron, L. *Molecular Light Scattering and Optical Activity*, 2nd ed.; Cambridge University Press: Cambridge, U. K., 2004.
(32) Hug, W. In *Handbook of Vibrational Spectroscopy*; Chalmers, J. M., Griffiths, P. R., Eds.; John Wiley and Sons: Chichester, U. K., 2002; pp 745−758.
(33) Ruud, K.; Thorvaldsen, A. J. *Chirality* **2009**, *21*, E54–E67.
(34) Liégeois, V.; Ruud, K.; Champagne, B. *J. Chem. Phys.* **2007**, *127*, 204105.
(35) Bast, R.; Ekström, U.; Gao, B.; Helgaker, T.; Ruud, K.; Thorvaldsen, A. J. *Phys. Chem. Chem. Phys.* **2011**, *13*, 2627–2651.
(36) Thorvaldsen, A. J.; Ruud, K.; Kristensen, K.; Jørgensen, P.; Coriani, S. *J. Chem. Phys.* **2008**, *129*, 214108.
(37) Thorvaldsen, A. J.; Ruud, K.; Jaszuński, M. *J. Phys. Chem. A* **2008**, *112*, 11942–11950.
(38) Furche, F. *J. Chem. Phys.* **2007**, *126*, 201104.
(39) Reiher, M.; Neugebauer, J. *J. Chem. Phys.* **2003**, *118*, 1634–1641.
(40) Luber, S.; Neugebauer, J.; Reiher, M. *J. Chem. Phys.* **2009**, *130*, 064105.
(41) Luber, S.; Reiher, M. *ChemPhysChem* **2009**, *10*, 2049–2057.
(42) Halls, M. D.; Schlegel, H. B. *J. Chem. Phys.* **1999**, *111*, 8819.
(43) Zuber, G.; Hug, W. *J. Phys. Chem. A.* **2004**, *108*, 2108–2119.
(44) Reiher, M.; Liegéois, V.; Ruud, K. *J. Phys. Chem. A* **2005**, *109*, 7567–7574.
(45) Bose, P. K.; Polavarapu, P. L.; Barron, L. D.; Hecht, L. *J. Phys. Chem.* **1990**, *94*, 1734–1740.
(46) Luber, S.; Herrmann, C.; Reiher, M. *J. Phys. Chem. B* **2008**, *112*, 2218–2232.
(47) Costante, J.; Hecht, L.; Polavarapu, P. L.; Collet, A.; Barron, L. D. *Angew. Chem., Int. Ed.* **1997**, *36*, 885–887.
(48) Che, J.; Nafie, L. A. *Chem. Phys. Lett.* **1992**, *189*, 35–46.
(49) Ruud, K.; Helgaker, T.; Bouř, P. *J. Phys. Chem. A* **2002**, *106*, 7448–7455.
(50) Barron, L. D.; Hecht, L.; Gargaro, A. R.; Hug, W. *J. Raman Spectrosc.* **1990**, *21*, 375–379.
(51) Yu, G. S.; Freedman, T. B.; Nafie, L. A. *J. Raman Spectrosc.* **1995**, *26*, 733–743.
(52) Stephens, P. J.; Devlin, F. J.; Cheeseman, J. R.; Frisch, M. J. *J. Phys. Chem. A* **2001**, *105*, 5356–5371.
(53) Ruud, K.; Stephens, P. J.; Devlin, F. J.; Taylor, P. R.; Cheeseman, J. R.; Frisch, M. J. *Chem. Phys. Lett.* **2003**, *373*, 606–614.
(54) Jean-Charles, K. L.; Camara, C.; Dumas, F. First Asymmetric Synthesis of Suberosenone and Suberosanone: Absolute Stereochemistry Assignment of Natural Suberosanes. Poster at Chirality 2004, the 16th International Symposium on Chirality, ISCD 16, New York.
(55) Stephens, P. J.; McCann, D. M.; Devlin, F. J.; Smith, I., A. B. *J. Nat. Prod.* **2006**, *69*, 1055–1064.
(56) Cheeseman, J. R.; Shaik, M. J.; Popelier, P. L. A.; Blanch, E. W. *J. Am. Chem. Soc.* **2011**.

(57) Bell, A.; Barron, L.; Hecht, L. *Carbohydr. Res.* **1994**, *257*, 11–24.
(58) Polavarapu, P. L.; Deng, Z. *Faraday Discuss.* **1994**, *99*, 151–163.
(59) Hug, W. *Chem. Phys.* **2001**, *264*, 53–69.
(60) Frisch, M. J.; Trucks, G. W.; Schlegel, H. B.; Scuseria, G. E.; Robb, M. A.; Cheeseman, J. R.; Scalmani, G.; Barone, V.; Mennucci, B.; Petersson, G. A.; Nakatsuji, H.; Caricato, M.; Li, X.; Hratchian, H. P.; Izmaylov, A. F.; Bloino, J.; Zheng, G.; Sonnenberg, J. L.; Hada, M.; Ehara, M.; Toyota, K.; Fukuda, R.; Hasegawa, J.; Ishida, M.; Nakajima, T.; Honda, Y.; Kitao, O.; Nakai, H.; Vreven, T.; Montgomery, J. A., Jr.; Peralta, J. E.; Ogliaro, F.; Bearpark, M.; Heyd, J. J.; Brothers, E.; Kudin, K. N.; Staroverov, V. N.; Keith, T.; Kobayashi, R.; Normand, J.; Raghavachari, K.; Rendell, A.; Burant, J. C.; Iyengar, S. S.; Tomasi, J.; Cossi, M.; Rega, N.; Millam, J. M.; Klene, M.; Knox, J. E.; Cross, J. B.; Bakken, V.; Adamo, C.; Jaramillo, J.; Gomperts, R.; Stratmann, R. E.; Yazyev, O.; Austin, A. J.; Cammi, R.; Pomelli, C.; Ochterski, J. W.; Martin, R. L.; Morokuma, K.; Zakrzewski, V. G.; Voth, G. A.; Salvador, P.; Dannenberg, J. J.; Dapprich, S.; Parandekar, P. V.; Mayhall, N. J.; Daniels, A. D.; Farkas, Ö.; Foresman, J. B.; Ortiz, J. V.; Cioslowski, J.; Fox, D. J. *Gaussian Development Version*, Revision H.09+; Gaussian, Inc.: Wallingford, CT, 2010.
(61) London, F. *J. Phys-Paris* **1937**, *8*, 397–409.
(62) Ditchfield, R. *Mol. Phys.* **1974**, *27*, 789–807.
(63) Hehre, W. J.; Ditchfield, R.; Pople, J. A. *J. Chem. Phys.* **1972**, *56*, 2257.
(64) Francl, M. M.; Pietro, W. J.; Hehre, W. J.; Binkley, J. S.; DeFrees, D. J.; Pople, J. A.; Gordon, M. S. *J. Chem. Phys.* **1982**, *77*, 3654–3665.
(65) Hariharan, P. C.; Pople, J. A. *Theor. Chem. Acc.* **1973**, *28*, 213–222.
(66) Clark, T.; Chandrasekhar, J.; Spitznagel, G. W.; Schleyer, P. v. R. *J. Comput. Chem.* **1983**, *4*, 294–301.
(67) Krishnan, R.; Binkley, J. S.; Seeger, R.; Pople, J. A. *J. Chem. Phys.* **1980**, *72*, 650.
(68) Gill, P. M. W.; Johnson, B. G.; Pople, J. A.; Frisch, M. J. *Chem. Phys. Lett.* **1992**, *197*, 499–505.
(69) McLean, A. D.; Chandler, G. S. *J. Chem. Phys.* **1980**, *72*, 5639–5648.
(70) Frisch, M. J.; Pople, J. A.; Binkley, J. S. *J. Chem. Phys.* **1984**, *80*, 3265–3269.
(71) Dunning, T. H., Jr. *J. Chem. Phys.* **1989**, *90*, 1007–1023.
(72) Kendall, R. A.; Dunning, T. H., Jr.; Harrison, R. J. *J. Chem. Phys.* **1992**, *96*, 6796–6806.
(73) Woon, D. E.; Dunning, T. H., Jr *J. Chem. Phys.* **1993**, *98*, 1358–1371.
(74) Sadlej, A. J. *Collect. Czech. Chem. C.* **1988**, 53.
(75) Sadlej, A. J. *Theor. Chem. Acc.* **1991**, *79*, 123.
(76) Baranowska, A.; Łączkowski, K. Z.; Sadlej, A. J. *J. Comput. Chem.* **2009**, *31*, 1176–1181.
(77) Schaefer, A.; Horn, H.; Ahlrichs, R. *J. Chem. Phys.* **1992**, *97*, 2571–2577.
(78) Schaefer, A.; Huber, C.; Ahlrichs, R. *J. Chem. Phys.* **1994**, *100*, 5829–5835.
(79) Ruud, K.; Skaane, H.; Helgaker, T.; Bak, K.; Jørgensen, P. *J. Am. Chem. Soc.* **1994**, *116*, 10135–10140.
(80) Lee, H.; Nafie, L. Private communication.
(81) Absolute Raman intensities and ROA intensity differences were not measured experimentally.
(82) Wiberg, K. B.; Wang, Y.; Vaccaro, P. H.; Cheeseman, J. R.; Trucks, G. W.; Frisch, M. J. *J. Phys. Chem. A* **2004**, *108*, 32–38.